

An ion ring in a linear multipole trap for optical frequency metrology

C. Champenois,* M. Marciante, J. Pedregosa-Gutierrez, M. Houssin, and M. Knoop

Physique des Interactions Ioniques et Moléculaires,

UMR 6633 CNRS et Aix-Marseille Université,

Centre de Saint Jérôme, Case C21, 13397 Marseille Cedex 20, France

M. Kajita

National Institute for Information and Communications Technology,

4-2-1, Nukui-Kitamachi, Koganei, Tokyo 184-8795, Japan

(Dated: February 22, 2019)

Abstract

A ring crystal of ions trapped in a linear multipole trap is studied as a basis for an optical frequency standard. The equilibrium conditions and cooling possibilities are discussed through an analytical model and molecular dynamics simulations. A configuration which reduces the frequency sensitivity to the fluctuations of the number of trapped ions is proposed. The systematic shifts for the electric quadrupole transition of calcium ions are evaluated for this ring configuration. This study shows that a ring of 10 or 20 ions allows to reach a short term stability better than for a single ion without introducing limiting long term fluctuations.

PACS numbers: 37.10.Ty (Ion trapping) 37.10.Rs (Ion cooling) 06.30.Ft (Time and frequency)

*caroline.champenois@univ-provence.fr

I. INTRODUCTION

Progress in atom and ion cooling and trapping, laser stabilization and high-resolution spectroscopy makes narrow optical transitions the best candidates for frequency standards. Three experimental systems take the optical clocks to their highest performances: a laser-cooled neutral atom cloud in a MOT [1, 2], an ensemble of laser-cooled neutral atoms in an optical lattice [3–5] and single trapped laser-cooled ions [6–9]. All systems have advantages and drawbacks. The main advantage of single ion experiments is the quasi-perfect control of the internal and external degrees of freedom, permitted by the trapping in radiofrequency (rf) electric fields in the quadrupole configuration. This ultimate control, possible only with a single particle, is paid for by a low signal-to-noise ratio which requires a long integration time, resulting in a small short term stability when compared to neutral atom optical clocks where 10^6 to 10^8 atoms are interrogated at the same time.

In the same time, microwave frequency standards with large clouds of trapped ions ($> 10^6$ ions) [10, 11] are developed to assure a good short term stability (characterized by an Allan deviation $\sigma_y(\tau) < 10^{-13}/\sqrt{\tau}$) and an excellent long term stability $\sigma_y(\tau) < 10^{-16}$ per day). In the context of deep space navigation [12], precision is not a major issue and a fractional frequency uncertainty of 10^{-11} is admitted to be sufficient. The main systematic effect which limits the long term stability is the second order Doppler effect induced by the rf driven motion (called micromotion). This effect depends on the size of the cloud through the maximum amplitude of the electric field seen by the ions and requires a high stability of the ion number over a long time scale. For an equal number of trapped ions, this shift is reduced by using linear multipole traps where the electric field amplitude is almost null in the center part of the trap [13]. Large ion samples can thus be trapped with reduced micromotion, compared to the quadrupole geometry. For a dense enough ion cloud, one can show [12] that the maximum second order Doppler shift $\delta f_{D2} = -f_0 \langle v^2 \rangle / (2c^2)$ simply writes

$$\delta f_{D2} = -f_0 \frac{q^2 N_L}{8\pi\epsilon_0 m(k-1)c^2}, \quad (1)$$

where f_0 is the frequency of the atomic clock transition, N_L is the number of ions per unit length, m is the mass of the ions, q their charge, $2k$ is the number of electrodes in the multipole trap and c the speed of light. The $(k-1)^{-1}$ scaling justifies the choice of a higher order multipole [14] for challenging clock applications. Indeed, in [12] a 16-pole trap is used to trap ions during the interrogation of their clock transition. Multipole rf traps are also widely used to study cold reactive collisions [15] as cooling with a buffer gas from 300 K to 4 K [16] allows to control the kinetic energy of the collisions and to reproduce astrophysical conditions.

Laser cooling and crystal structures of cold ions in multipole traps are far less studied than in quadrupole traps. Laser cooling and observation of ion crystals in a linear octupole trap have been reported in [17, 18]. A semi-analytical and numerical study of the structure, scaling laws and phase transitions of cold ions in an isotropic 3D octupole can be found in [19]. These two studies show that a cold ion cloud can be described as a hollow core system, resulting from the balance between the Coulomb repulsion and a trapping potential nearly flat in the center and very steep at the border. Such a geometry can be also deduced by a cold fluid model [20]. When the number of trapped ions is reduced to the order of 100 or less, simulations show that, for certain trapping parameters, the tube formed by the ions reduces to a ring crystal centered on the symmetry axis.

In this article, we propose to use laser-cooled ions trapped in a linear multipole rf trap and organized in a ring structure as a basis for an optical clock. The aim is not to compete with the highest precision a single ion optical clock can offer, but to propose a trade-off where a somewhat lower precision is compensated by a gain in short term stability offered by the interrogation of several ions at the same time. The main technological challenge in the realization of a single ion frequency standard is the clock laser which has to reach frequency stabilities of the order of 1 Hz/s. The present proposal allows to reach total clock performances comparable to a single-ion experiment by relaxing the constraints on the laser performance by at least one order of magnitude. The improvement can be illustrated by the Allan variance which is used to quantify the stability :

$$\sigma_y(\tau) = \frac{1}{\pi Q(SNR)} \sqrt{\frac{T_c}{\tau}}, \quad (2)$$

with Q the quality factor of the measured transition, (SNR) the signal-to-noise ratio of the excitation probability measurement and T_c the cycle time required to build an atomic signal to counteract on the laser frequency. The (SNR) is limited by the quantum projection noise [21] to \sqrt{N} and using $N = 10$ or 20 ions allows to reach the same stability value 10 or 20 times faster than a single ion clock, if the line is not broadened.

Compared to a chain of ions in a linear quadrupole trap, this ring configuration has the advantage of having the same symmetry as a transverse laser beam intensity profile assuring that every ion sees the same laser intensity. The second advantage of this symmetry is that the motion along the trap axis is characterized by a single oscillation frequency. Furthermore, the trapping parameters can be chosen to constrain the radial size of the ring, independent from the number of trapped ions, to first order (if this number obeys some stability conditions). As a consequence, the possible loss of one ion during long time operation induces only a second order perturbation on the ring equilibrium radius and causes very small frequency fluctuations. The compactness and the symmetry of a ring compared

to a chain made of the same number of ions is another advantage regarding the dispersion of the systematic shifts induced by local electric or magnetic fields.

The planar crystal structure of the present study could also be of use for quantum computation experiments. Planar crystals in a quadrupole trap are proposed in [22] as an appropriate system for large scale quantum computation and their structure is studied in [23] by molecular dynamics simulations. The ring configuration we propose here for trapped ions could also be used for quantum simulations like demonstrated in [24] with several Rydberg atoms at each site, to investigate many-body quantum states.

In the following section, we start by describing the features concerning the trapping and cooling of the sample, relevant for an optical clock of this kind. We then identify two configurations that obey the clock operation conditions: a ring of 10 ions and one of 20 ions. In section III, the scaling laws and numerical values of the systematic shifts due to the ring configuration are given. In a second step (section IV), the systematic shifts usually encountered by a single ion clock are estimated for this ring configuration. In the last part, all contributions are summarized to propose an uncertainty budget for the 10- and for the 20-ions ring clock. The numerical calculations quantifying all the effects use the optical quadrupole transition of $^{40}\text{Ca}^+$ as the clock transition [25, 26] and are carried out for a linear octupole trap ($2k = 8$). However, most of the equations can be transposed to other species and to higher order traps.

II. SELF-ORGANIZATION OF IONS IN A RING

In the adiabatic approximation, the static pseudopotential associated to the rf electric field allows to explain the dynamics and equilibrium positions of the ions in the transverse plane of the trap. For a perfect linear multipole trap of order $2k$, it is defined like [15]

$$V^*(r) = \frac{k^2 q^2 V_0^2}{16m\Omega^2 r_0^2} \left(\frac{r}{r_0} \right)^{2k-2}, \quad (3)$$

where r is the ion distance to the trap axis, V_0 is the amplitude of the rf potential difference between two neighbouring electrodes, $\Omega/2\pi$ the frequency of this applied voltage and r_0 the inner radius of the trap. To effectively trap the ions, a static potential has to be applied on electrodes placed on both ends of the linear trap. This geometry creates a potential well along the axis of symmetry Oz which we can consider as harmonic in the centre of the trap. The full contribution of this static potential can be written like

$$V_{stat} = \frac{1}{2} m \omega_z^2 \left(z^2 - \frac{r^2}{2} \right) \quad (4)$$

where the harmonic well is characterized by the oscillation frequency ω_z . When the multipole is not a quadrupole ($2k \neq 4$), the two contributions $V^*(r)$ and V_{stat} for the trapping potential

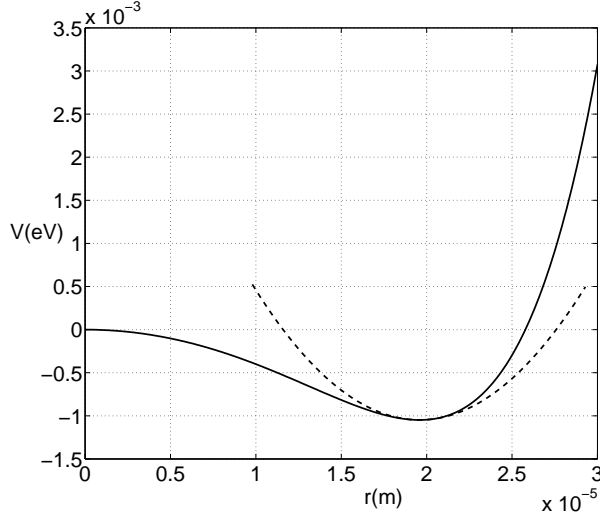


FIG. 1: Solid line: effective static potential (in eV) in the radial plane of an octupole trap ($2k = 8$), resulting from the contributions of $V^*(r)$, V_{stat} . Dashed line: the harmonic approximation of the potential well defined by r_{min} (Eq. 5) and ω_{eff} (Eq. 8). The potentials are defined by $\omega_z/2\pi = 1$ MHz, $\Omega_z/2\pi = 20$ MHz, $V_0 = 394.4$ V and $r_0 = 200$ μm , for calcium ions ($m = 40$ a.m.u.).

result in a potential shape (solid line in figure 1), where the minimum is shifted from $r = 0$ to $r = r_{min}$ defined by

$$r_{min}^{2k-4} = \frac{1}{k-1} \left(\frac{2m\Omega\omega_z r_0^k}{kqV_0} \right)^2. \quad (5)$$

A. Equilibrium

The equilibrium position of a set of ions results from the balance between the Coulomb repulsion and the trapping potential. An analysis of the forces along the radial direction shows that two regimes of organization can be defined, based on the strength of the deconfinement contribution $-m\omega_z^2 r^2/4$ compared to the Coulomb repulsion induced on an ion at radial distance R by all the other ions. In the assumption of a ring of radius R in a single plane, the Coulomb potential energy for a set of N ions $E_p^C(N)$ is

$$E_p^C(N) = \frac{q^2}{4\pi\epsilon_0} \frac{N}{2} \frac{S_1(N)}{2R} \quad (6)$$

with $S_1(N) = \sum_{n=1}^{N-1} 1/\sin(\pi n/N)$. If this contribution is negligible compared to the deconfinement, the radius of equilibrium R does not depend on the number of ions N . In the

prospect of a clock where the major systematic shifts depend on the equilibrium position R through the local rf electric field, this condition has to be fulfilled to allow the ion number not to be strictly reproduced from day to day. In the following, we consider that the configuration is such that, at first order of approximation, the equilibrium position R is given by the minimum potential r_{min} defined by Eq. 5 and does not depend on the number of ions in the ring. The Coulomb repulsion can be treated as a perturbation and the radial position shift ϵ that it induces depends on various trap parameters like

$$\epsilon = \frac{q^2}{4\pi\epsilon_0} \frac{S_1(N)}{4(k-2)r_{min}^2 m\omega_z^2}. \quad (7)$$

With the ion number N and ring radius considered in the following, the relative Coulomb shift ϵ/r_{min} is smaller than 0.02, justifying the assumption that $R \simeq r_{min}$ to deduce the scaling laws for the systematic shifts.

With the typical trapping parameters used through this article, local potential depths equivalent to 10 K can be made while temperatures as low as 10 mK can be reached in the radial direction by Doppler laser cooling. Laser cooled ions will settle in the bottom of this well and at this level, the radial pseudopotential can be approximated by a harmonic potential centered on r_{min} (see Figure 1). An analytical analysis shows that the second order expansion of the radial potential around r_{min} , $V^*(r) + V_{stat}(r) \simeq V^*(r_{min}) + V_{stat}(r_{min}) + m\omega_{eff}^2(r - r_{min})^2/2$, is characterized by an effective oscillation frequency ω_{eff} which depends only on the axial frequency and the order of the multipole by

$$\omega_{eff} = \sqrt{k-2} \omega_z. \quad (8)$$

This shows that the strength of the axial trapping ω_z also defines the strength of the radial trapping around the equilibrium position R .

To make relevant predictions based on the pseudopotential (Eq 3), the adiabatic approximation at position r_{min} has to be satisfied. Contrary to quadrupole traps, there is no absolute criterion for adiabatic operation of the multipole trap. However, the Mathieu parameter q_x used in quadrupole traps to characterize the trajectories of ions can be generalized to multipole with the main difference that this new parameter η depends on the ion's location in the trap [15, 27]. For a perfect multipole, this parameter is defined like

$$\eta(r) = k(k-1) \frac{qV_0}{m\Omega^2 r_0^2} \left(\frac{r}{r_0} \right)^{k-2} \quad (9)$$

and has been empirically limited to 0.3 to guarantee stability of the trajectories [15]. A more recent experimental study of the loss mechanism in a 22-pole trap [28] complementary to a model of effective trapping volume [29] has demonstrated stability up to $\eta(r) < 0.36 \pm 0.02$.

Moreover, clock operation requires also a small micromotion amplitude to limit all the systematic effects induced by this motion and to minimize the rf heating that may occur, as in quadrupole traps. For this reason, and by analogy with linear quadrupole traps, we limit the set of trapping parameters to keep $\eta < 0.2$. For a ring of ions at a distance $R = r_{min}$ from the center and including Eq. 5 into Eq. 9, the adiabatic parameter takes the simple form

$$\eta(R) = 2\sqrt{k-1}\frac{\omega_z}{\Omega} \quad (10)$$

which does not explicitly depend on the equilibrium position nor on the number of ions, and immediately fixes the range of the trapping frequency $\Omega/2\pi$ once the axial oscillation frequency is chosen. Indeed, in an octupole trap with $\omega_z/2\pi = 1$ MHz, it takes $\Omega/2\pi > 17$ MHz to assure $\eta < 0.2$. Furthermore, the amplitude of the micromotion δR_μ also scales like $\eta(R)$ but increases with the distance to the center like

$$\delta R_\mu = R\eta(R)\frac{1}{2(k-1)}. \quad (11)$$

Therefore, a radial equilibrium position as small as possible is chosen, to reduce the induced heating as well as the rf induced systematic shifts, which depend on the local rf electric field and scale like R^{k-1} . The lower limit of this radius is set by the ion-ion distance. For a distance too small, the one ring configuration is not stable and the system relaxes to a double ring where the sum of the Coulomb and trapping potential energies is lower. Simple energy minimization, confirmed by molecular dynamics (MD) simulations, shows that in a double ring of an even number of ions, the ions alternate from one ring to the other in a configuration analog to the zig-zag chain already observed in a quadrupole linear trap [30] (see Figure 2). Writing the equilibrium condition along Oz for a double ring of N ions requires that R should be smaller than a limit R_l , which sets the lower stability limit for a one-ring configuration. This limit size depends only on the strength of the axial potential and the number of ions as

$$R_l = \left(\frac{q^2/4\pi\epsilon_0}{4m\omega_z^2}\right)^{1/3} \left(\sum_{n=1}^{N/2} \frac{1}{\sin^3 \frac{(2n-1)\pi}{N}}\right)^{1/3} \simeq \left(\frac{q^2/4\pi\epsilon_0}{2m\omega_z^2}\right)^{1/3} \frac{N}{\pi}. \quad (12)$$

and therefore scales like N .

B. Doppler cooling

So far, we have been concerned by the static properties of the ring configuration. In this second section, we focus on the thermodynamic issues related to ion temperature required

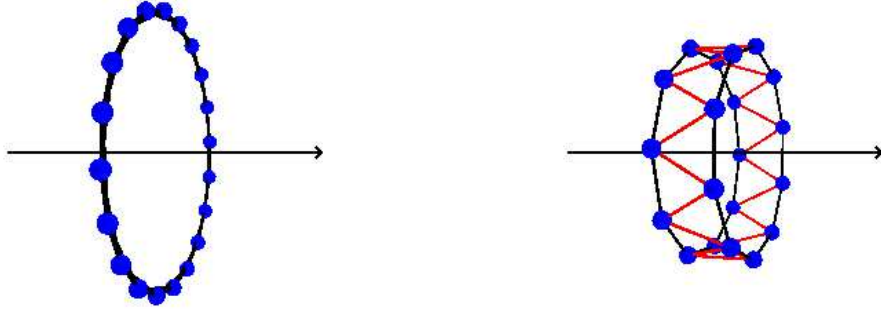


FIG. 2: (Color online) Equilibrium position of 20 calcium ions around the trap symmetry axis, calculated by MD simulations in the pseudo-potential of a linear octupole trap. The potential is defined by $\omega_z/2\pi = 1$ MHz and $\Omega_z/2\pi = 20$ MHz and for 20 ions, the stability limit is $R_l = 23\mu\text{m}$. Left: $V_0 = 3142$ V and $r_0 = 400\mu\text{m}$, resulting in $r_{min} > R_l$, the one ring configuration is stable ($R = 28\mu\text{m}$). Right: $V_0 = 5771$ V and $r_0 = 400\mu\text{m}$, resulting in $r_{min} < R_l$, the stable configuration is a double ring analog to a closed zig-zag chain. Here the separation between the two planes is of the order of $3\mu\text{m}$ and their radius is $21\mu\text{m}$.

for clock operation. We first introduce these requirements and their consequences for the geometry of the set-up and then propose two configurations that fulfill these requirements.

When the trapping parameters are adjusted to obtain a single ring of ions lying in the $z = 0$ plane, it seems mandatory to propagate the clock laser along the Oz direction, such that no line broadening is introduced by dispersion of the excitation strength on the clock transition from one ion to another. In this configuration, there is no micro-motion along the laser axis and the first order Doppler effect is sensitive only to the thermal motion along the axial direction (called macro-motion). To compete with the existing clocks, this effect has to be canceled. The method used for trapped ion frequency standards is to set the ion motion in the Lamb-Dicke regime where the phase modulation induced by the ion motion inside the clock laser wave is small compared to 2π . For optical transitions, the wavelength is so small that laser cooling is required to reach that stage. One of the major issues of laser cooled ion trap design is to make sure that the Lamb-Dicke regime can be reached by Doppler laser cooling so that no other laser cooling process is required for clock operation [31].

When the ion motion can be described by an harmonic oscillation $Z \cos \omega_z t$, a classi-

cal expansion of the laser-atom interaction [32] shows that the Doppler spectrum can be understood like the superposition of sidebands at frequency $f_0 \pm n\omega_z/2\pi$ with amplitude proportional to $|J_n^2(k_L Z)|$, if the transitions are not saturated. J_n is the Bessel function of order n and the modulation index $k_L Z$ depends on the clock laser wavevector k_L and the amplitude of oscillation $Z = V_Z/\omega_z$. The velocity amplitude of the oscillation V_Z depends on the temperature reached by the cooling T_z . When the Doppler laser cooling limit is reached, $V_Z = \sqrt{\hbar\gamma/m}$ where γ is the spontaneous decay rate on the cooling transition (at 397 nm for calcium ion). For the Ca^+ clock transition at 729 nm with ions at the Doppler limit T_D ($T_D = 0.54$ mK, with $1/\gamma = 7 \times 10^{-9}$ s), the modulation index is $2\pi \times 6.3 \times 10^5/\omega_z$. Choosing $\omega_z/2\pi = 1$ MHz is sufficient to assure a modulation index smaller than 1 which sets the motion in the Lamb-Dicke regime and leads to a central band nearly 10 times stronger than the first oscillation sidebands, which is a good enough operation condition for an optical clock[25]. We will see later in the text that further increase of the axial oscillation frequency is detrimental to the performances of the clock and the chosen value appears to be a good compromise between a small oscillation amplitude and small systematic shifts.

All the considerations introduced in the previous part about the equilibrium position of the ions inside the pseudopotential are not sufficient to control the dynamics of the set of ions. To get more insight in the system, molecular dynamics (MD) is used to simulate the ion motion under Coulomb repulsion and laser cooling, in the full rf potential

$$\Phi_k(\mathbf{r}, t) = V_0/2 \cos(\Omega t)(r/r_0)^k \cos(k\alpha) \quad (13)$$

where (r, α) are the polar coordinates in the (x, y) plane. Details of these simulations will be published elsewhere [33]. These simulations show that in the single ring configuration, the axial and radial degrees of freedom are very weakly coupled and the thermal equilibrium of each degree is characterized by very different temperatures. With laser cooling on the three directions of space, the simulations show that for a decoupled system, the Doppler limit temperature is reached in the axial direction and the temperatures in the radial plane (T_r, T_α) reach 10 mK in the best configuration (laser detuning set at $-\gamma/2$ and coupling strength defined by a Rabi frequency equal to $\gamma/2$). The MD simulations show that if the trapping parameters result in a radius of the ring too close to the stability limit R_l , the axial and radial degrees of freedom are coupled and the temperature for the axial motion does not reach the Doppler limit. Reaching the Doppler limit in the axial direction is mandatory for the Lamb-Dicke regime, and we can design potentials able to trap a ring made of 10 to 100 ions in a single plane, fulfilling this condition.

For clock operation additional conditions have to be fulfilled. Indeed, to prevent light-shift on the clock transition, the cooling lasers must not be applied onto the ions during the clock transition excitation [25]. During this excitation, which needs to last at least several

milliseconds, the system must remain at the same temperature. With simulations, we have found trapping and cooling conditions compatible with these requirements only for rings smaller than 20 ions. The 100-ions ring heats up very fast and, in the best configuration, the axial temperature increases from 0.54 mK (the Doppler limit) to 2 mK in 1 ms. This rapid increase is due to rf heating as the micromotion amplitude increases with R (see Eq. (11)) which increases like N . On the contrary, for 10 ions set in a ring of radius 20 μm or for 20 ions set in a ring of radius 40 μm , the cooling laser can be switched off for several ms with very little heating. To reach good statistics we build a sequence of 2 ms of dark time (the clock interrogation) followed by 2 ms of laser cooling, and measure the temperature throughout the dark times. For the 10-ions ring, after 120 periods of cooling/non cooling time, the average axial temperature is 0.47 mK and the FWHM of the distribution is 0.32 mK. Clock operation conditions for a 10-ions ring can thus be fulfilled (similar results can be obtained for the 20 ion ring). For comparison, all the configurations have the same axial and rf frequency $\omega_z/2\pi = 1$ MHz, $\Omega/2\pi = 20$ MHz, and therefore the same adiabatic coefficient at the position of the ions $\eta(R) = 0.17$. The ring radius was controlled by the amplitude of the rf electric field.

The constraints on the trapping parameters and their relation can be summarized as follows: the minimum value of ω_z is fixed by the Lamb-Dicke regime. Once ω_z chosen, the value of Ω is fixed by the adiabacity criteria (Eq. 10). Then, for a given number of trapped ions N , the ratio V_0/r_0^4 is chosen to match r_{min} with the smallest R that allows to keep the ions in a single ring ($R > R_l$) which does not heat up when the cooling lasers are off. The MD analysis shows that it is possible to form a stable ring of 10 to 20 ions, with a temperature close to the Doppler limit in the axial direction and of the order of 10 mK in the radial direction. In the second part of this paper we evaluate frequency shifts on the clock transition for two configurations tested by MD simulations : a 10-ions ring of radius 20 μm and a 20-ions ring of radius 40 μm . With the chosen trapping frequencies, it takes $V_0 = 394$ V for $r_0 = 200$ μm to reach $R = 20\mu\text{m}$ and $V_0 = 1578$ V for $r_0 = 400$ μm to reach $R = 40\mu\text{m}$. Furthermore, we assume an axial temperature of 0.54 mK (the Doppler limit T_D for calcium ion) and a radial temperature T_r of 10 mK. This temperature controls the thermal motion amplitude along the radial direction δR through

$$\delta R = \sqrt{\frac{2k_B T_r}{m(k-2)\omega_z^2}} \quad (14)$$

and is responsible for line broadening through every systematic shift depending on the radial position R . To give an order of magnitude of this effect, for calcium ions in a linear octupole trap with $\omega_z/2\pi=1$ MHz, the thermal motion amplitude in the radial direction δR is 0.23 μm , to be compared to the amplitude of the micro-motion δR_μ which is 0.56 μm for a 20 μm

radius (and $1.1 \mu\text{m}$ for a $40 \mu\text{m}$ radius). These equilibrium and dynamic properties control several systematic shifts which are discussed in the following section.

III. SYSTEMATIC SHIFTS INDUCED BY THE RF ELECTRIC FIELD

Compared to a single ion experiment, additional systematic shifts are introduced by the fact that the rf electric field is not null at the ion's equilibrium position. In this section, we focus on these extra effects and highlight their scaling law to point out the best compromise for a clock operation. The performances of a clock are evaluated by its accuracy and stability and the laws scaling their dependance with the number of ions are different. For every shift depending on the equilibrium position R (which scales with N to obey the equilibrium condition $R > R_l$), there is a line broadening induced by the thermal oscillation amplitude δR (which does not depend on N) and a long term fluctuation induced by the possible loss of one ion. This last effect depends on $\Delta\epsilon = \epsilon(N) - \epsilon(N-1)$ which scales with $1/N^2$. All shifts are evaluated for the quadrupole transition at 729 nm ($S_{1/2}, M_J \rightarrow D_{5/2}, M'_J$) of a $^{40}\text{Ca}^+$ ion which has no hyperfine structure. The trapping frequency is chosen to be $\Omega/2\pi = 20 \text{ MHz}$, with an axial confinement of $\omega_z/2\pi = 1 \text{ MHz}$.

A. Micromotion induced second order Doppler effect

The second order Doppler shift induced by the micro-motion is known to be the limiting factor for microwave ion clocks in multipole traps. The velocity amplitude of the micromotion V_μ is equal to $\Omega\delta R_\mu$ and the shift induced on the clock transition frequency f_0 , can be expressed like

$$\delta f_{D2} = -f_0 \frac{\omega_z^2 R^2}{4(k-1)c^2}. \quad (15)$$

In analogy to large clouds in a multipole trap (Eq. (1)), this shift scales with $1/(k-1)$, pleading for higher order multipole traps. But contrary to large clouds, the shift does not depend explicitly on the number of trapped ions but only on the trapping parameters, which can be very well controlled. The compromise to make for a clock operation is clearly visible from Eq. (15) : the reduction of the second order Doppler shift asks for ω_z and R values as small as possible whereas the ion ring stability and cooling set a lower limit to these two parameters.

For a ring of radius $20\mu\text{m}$ (respectively $40\mu\text{m}$) in an octupole trap ($k=4$), the shift is $1.46 \times 10^{-14} \times f_0 = 6.0 \text{ Hz}$ (respectively $5.85 \times 10^{-14} \times f_0 = 24.1 \text{ Hz}$) on the 729 nm optical clock transition of Ca^+ . The shift itself does not reduce the precision and stability of the clock, but its uncertainty and fluctuations can.

The slow (on the rf time scale) thermal oscillation of the ions in the radial plane is responsible for a dispersion in the radial position $\pm\delta R$ and implies a broadening of the second order Doppler shift $\Delta\delta f_{D2} = \pm\delta f_{D2}2\delta R/R$ (full width), which scales like $\omega_z R$, which itself is proportional to N and is lower than one Hertz with the typical parameters we have chosen ($\Delta\delta f_{D2} = \pm 3.4 \times 10^{-16} \times f_0 = \pm 0.14$ Hz for $R = 20\mu\text{m}$ and $\pm 6.7 \times 10^{-16} \times f_0 = \pm 0.28$ Hz for $R = 40\mu\text{m}$).

In long term operation, an ion can be lost and the shift in the radial equilibrium position $\Delta\epsilon$ induces a modification of the frequency shift equal to $\delta f_{D2}2\Delta\epsilon/R$, which scales like $1/N$. For the 10 ion ring of radius $20\mu\text{m}$, the fractional fluctuation is $8.5 \times 10^{-17} \times f_0 = 0.03$ Hz and it is $5.1 \times 10^{-17} \times f_0$ for a 20 ion ring of radius $40\mu\text{m}$. One can see that the 10^{-16} threshold we aim at for the long term stability can already be reached with a ring configuration of 10 ions. Increasing the number of ions decreases the long term fluctuations.

B. Stark effect induced by the electric trapping fields

The Stark effect results from the contribution from a scalar shift, which is proportional to the square amplitude of the electric field $E_{rf}^2/2 + E_{dc}^2$ (the 1/2 being due to the time averaging of the rf component) and a contribution from a tensorial part, which is sensitive to the angle between the magnetic field and the electric field at the position of the ion [34]. The scalar and tensorial shifts are proportional to the differential polarizability between the upper and lower states of the clock transition and the scalar contribution $\Delta\alpha^0 = -1.1 \times 10^{-6}$ Hz/(V/m)² [35] is independent of their Zeeman sublevels. For calcium ions, the tensorial contribution is of the same order of magnitude than the scalar one [25, 26, 35] and depends on the Zeeman sublevels M_J chosen for the $D_{5/2}$ state (the $S_{1/2}$ state has no contribution to the tensorial shift): $\Delta\alpha^2 = -6.1 \times 10^{-7} \times f(M_J)$ Hz/(V/m)² [35] with $f(M_J = \pm 1/2) = -4/5$, $f(M_J = \pm 3/2) = -1/5$ and $f(M_J = \pm 5/2) = 1$.

The amplitude of the rf electric field is deduced from Eq. (13) and for ions at distance R from the center, matching the potential minimum r_{min} , its contribution to the scalar Stark shift can be written like

$$\delta f_S^0(rf) = -\frac{1}{2}\Delta\alpha^0 \frac{m^2}{2(k-1)q^2} \omega_z^2 \Omega^2 R^2. \quad (16)$$

The scalar Stark shift induced by the dc electric field can be expressed with respect to the rf contribution :

$$\delta f_S^0(dc) = \delta f_S^0(rf) \frac{(k-1)\omega_z^2}{2\Omega^2} = \delta f_S^0(rf) \frac{\eta^2(R)}{8}. \quad (17)$$

This relation clearly shows that for $\eta(R) \leq 0.2$, the contribution from the dc field is negligible compared to the rf field contribution. As the Coulomb repulsion is small compared to the

dc radial electric field, the Stark effect induced by the Coulomb interaction is negligible compared to the dc contribution, which is itself negligible compared to the rf contribution. Therefore, only the rf contribution is taken into consideration in the uncertainty budget.

Like the second order Doppler shift (Eq. 15), the Stark effect scales with $1/(k-1)$ and is proportional to $\omega_z^2 R^2$. The new parameters that are introduced in the shift dependence are the mass of the ion and the trapping frequency. With the same parameters as mentioned before, $\delta f_S^0(rf) = 1.0 \times 10^{-14} \times f_0 = 4.1$ Hz and the line broadening induced is $\pm 2.3 \times 10^{-16} \times f_0 = \pm 0.09$ Hz for the ring radius of $20 \mu\text{m}$. For the ring radius of $40 \mu\text{m}$, the shift $\delta f_S^0(rf)$ is $4.0 \times 10^{-14} \times f_0 = 16.5$ Hz and the induced broadening is $\pm 4.6 \times 10^{-16} \times f_0 = \pm 0.19$ Hz. The fractional long term instability induced by $\Delta N = -1$ is 5.8×10^{-17} for the 10 ion ring of radius $20 \mu\text{m}$ (and 3.5×10^{-17} for the 20 ion ring of radius $40 \mu\text{m}$).

The tensorial Stark shift induced by the rf electric field depends on the angle θ between the local electric field and the magnetic field like [34]

$$\delta f_S^2(rf) = -\frac{1}{2} \Delta \alpha^2 f(M_J) \frac{3 \cos^2 \theta - 1}{2} \frac{E_{rf}^2}{2}. \quad (18)$$

In an rf trap, the amplitude of the rf electric field is constant over a ring but its direction rotates in the radial plane. The projection of this electric field on a static frame is defined by $(\cos(k-1)\alpha, \sin(k-1)\alpha)$ if α is the angle between the ion radial direction and a reference axis chosen in the radial plane. If the geometric configuration is such that θ varies from one ion to the other, the dispersion of the Stark shift induces a line broadening of the order of 1 Hz for the $20 \mu\text{m}$ radius ring and of 4 Hz for the $40 \mu\text{m}$ radius ring. Such a broadening, which is bigger than any other broadening calculated so far, can be avoided by choosing a magnetic field oriented along the trap axis ($\theta = \pi/2$), to assure the same Stark shift for all the ions of the ring. In this configuration and with the same trapping parameters, the tensorial Stark effect is $\delta f_S^2(rf)/f(M_J) = -0.3 \times 10^{-14} \times f_0 = -1.1$ H, with a line broadening $\pm 0.6 \times 10^{-16} \times f_0 = \pm 0.02$ Hz, for the ring radius of $20 \mu\text{m}$ ($\delta f_S^2(rf)/f(M_J) = -1.1 \times 10^{-14} \times f_0 = -4.6$ Hz with a broadening of $\pm 1.3 \times 10^{-16} \times f_0 = \pm 0.05$ Hz for the ring radius of $40 \mu\text{m}$). For the first case, the fractional long term frequency fluctuation induced by the loss of one ion is $1.4 \times 10^{-17} \times f(M_J)$ and is in the 10^{-18} range for the larger ring. The choice of the Zeeman sublevel used for the clock operation results from a compromise between several shifts, including the Zeeman shift itself. In the next section we present these effects that are not directly related to the trapping electric field.

IV. OTHER SYSTEMATIC SHIFTS AND THEIR DISPERSION

A. Zeeman effect

The selection rules for a quadrupole transition forbid $\Delta M_J = 0$ transition when the magnetic field lies along the direction of propagation of the clock laser. As the magnetic field is chosen along the trap symmetry axis to prevent the dispersion of the tensorial Stark shift, the use of $\Delta M_J = 0$ transitions would require an angle between the trap axis and the direction of propagation of the laser. This option has to be rejected because of the large Doppler effect induced by the rf driven motion. As a second choice, the $\Delta M_J = \pm 1$ transitions are allowed when the laser propagates along the magnetic field direction. Indeed, the $(S_{1/2}, M_J = \pm 1/2 \rightarrow D_{5/2}, M_J = \mp 1/2)$ transitions are only four times more sensitive to magnetic field fluctuations than their $(S_{1/2}, M_J = \pm 1/2 \rightarrow D_{5/2}, M_J = \pm 1/2)$ counterparts. The summation of the frequency of the two transitions $(S_{1/2}, M_J = \pm 1/2 \rightarrow D_{5/2}, M_J = \mp 1/2)$ should cancel the first order Zeeman shift if the magnetic field is constant in time at every point of the ring. A field fluctuation δB induces an uncertainty and a line broadening on this transition of 2.2 MHz/G. From the frequency fluctuations evaluated in [36] for the JPL Hg^+ microwave clock, and reached by a three layer magnetic shielding, one can infer magnetic field fluctuations of the order of 6×10^{-7} G, for a magnetic field of 0.05 G.

The magnetic field has to be large enough to resolve the transitions between various Zeeman sublevels. In a Ca^+ experiment, having a 1 kHz separation between neighboring transitions requires a magnetic field of 6×10^{-4} G. If one assumes the relative stability demonstrated in the JPL microwave clock, the Zeeman shift fluctuations are of the order of 0.013 Hz which result in a fractional uncertainty of 3×10^{-17} . If the same absolute stability can be reproduced, the Zeeman shift fluctuations reach 1.0 Hz which is equivalent to a fractional uncertainty of 2.5×10^{-15} . The same degree of frequency stability can be reached with less stringent conditions on the magnetic field stability using the hyperfine transition $M_F = 0 \rightarrow M'_F = 0$ of the odd isotope $^{43}\text{Ca}^+$ [25, 26]. Nevertheless, cooling and state detection with an odd isotope require more laser sources than with an even isotope and this complexity may not be acceptable.

The Zeeman effect also reduces the stability of a single ion cloud. The main difference here is that the magnetic field has to be kept constant and homogeneous over the 40 μm (or 80 μm) of the ring diameter, compared to the 1 μm scale associated to a single ion. This is still a favorable condition compared to the several centimeters long cloud used at JPL.

B. Blackbody radiation shift

The blackbody radiation shift (BBR shift) is the Stark effect induced by the thermal electric field radiated by the vacuum vessel and every part inside it. For calcium ions, very precise theoretical calculations [35] for the polarizabilities implied in the BBR shift allow to know the shift to better than 3%: $\delta f_{BBR} = 0.38(1)$ Hz. This result assumes that the radiated field is isotropic and that the temperature of the emitting surface is 300 K. As the BBR shift scales with T^4 , thermal fluctuations can be detrimental to high precision clocks. A 10 K uncertainty keeps the frequency uncertainty and eventual broadening (less probable as the time scales involved are very long) at the 0.05 Hz level, which is negligible in the context of our clock project. In conclusion, for temperature fluctuations smaller than 10 K a long term instability lower than 10^{-16} can be reached.

C. Quadrupole shift

Another effect well known in single ion optical clocks is the quadrupole shift induced by the gradient of the local electric field coupled to the electric quadrupole of the $D_{5/2}$ state (a $S_{1/2}$ state has none). Thanks to a recent experiment [37], in agreement with precise theoretical calculations [38], the quadrupole of the Ca^+ $D_{5/2}$ state is known to better than 1%: $\theta(D_{5/2}) = 1.83(1) ea_0^2$ (atomic unit). The coupling with the rf electric field gradient gives rise to sidebands in the clock transition spectra that are well separated from the central band f_0 , so that the dc electric field gradient is the only relevant contribution for this shift. The dc trapping field has a quadrupole profile and using the notation of [34], its gradient is $2A = -m\omega_z^2/(2q)$. For a magnetic field parallel to the trap symmetry axis and for $\omega_z/2\pi = 1$ MHz, the quadrupole shift is

$$\delta f_Q = 1.0 \times (3M_J^2 - 35/4) \text{ Hz.} \quad (19)$$

For the Zeeman sublevels $M_J = \pm 1/2$, the quadrupole shift induced by this dc trapping field is 8.0 Hz and does not depend on the position of the ions. If the axial trapping voltage is well controlled, this shift should not reduce the performance of the clock. It is not the case for the shift induced by extra dc fields which can build up in the trap, for example by neutral atom deposition. These fields can easily induce shifts of the order of 1 Hz from day to day operation and are well known from single ion clock operation. Two methods are used to reduce their day to day fluctuations: ionizing the neutral beam far from the clock operation area before shuttling them and/or using photoionization [39, 40] which requires a far smaller flux of neutrals than the traditional electron bombardment method. If required, the shift itself can be compensated by the combination of three measurements on different

Zeeman sublevels [41]. The method based on frequency measurements with three orthogonal directions of the magnetic field, used for single ion standard [6, 34], can not be applied here because of the tensorial Stark shift dispersion (see III B). All together, the uncertainty and fluctuations induced by this quadrupole shift must be made smaller than 0.04 Hz to keep the long term fractional frequency fluctuations smaller than 10^{-16} .

D. Misalignment

If the propagation axis of the clock laser does not match the symmetry axis of the ring, the ions do not see the same laser power. The induced variations in the excitation probability contribute to the noise of the excitation detection and reduce the short term stability of the clock. Assuming a single Rabi pulse to interrogate the clock transition and a maximum excitation probability on resonance ($\Omega_L T = \pi$ with Ω_L the Rabi frequency of the atom-laser coupling and T the pulse duration), the variation in the excitation probability for a detuning giving the maximum sensitivity is $\delta P_e(T) = 0.72\delta\Omega_L/\Omega_L$. If one considers a Gaussian laser beam of waist w_L and intensity profile $I_L(r) = I_0 \exp(-2r^2/w_L^2)$, one can connect the variation $\delta\Omega_L$ to a misalignment δr . The dispersion in the probability of excitation is then

$$\delta P_e(T) = 0.36 \frac{4r\delta r}{w_L^2}. \quad (20)$$

The quantum projection noise $1/2\sqrt{N}$ [21] is a fundamental limit which can only be beaten by entanglement and squeezing methods [42]. Making $\delta P_e(T)$ small compared to this noise is sufficient to make misalignment effects negligible. An easy solution is to make the laser waist a lot larger than the ring radius R . Already with $w_L = 2R$, a geometrical precision of $\delta r < 0.27R$ is enough to keep $\delta P_e(T) < 0.1$ and makes the contribution to the noise negligible.

V. CONCLUSION

The shift and uncertainty budget presented in table I shows that the rf is responsible for the major shifts and broadenings. The total broadening of the transition is smaller than 1 Hz, which is smaller than or comparable to the spectral broadening induced by the finite time excitation on the clock transition, depending on the Rabi pulse duration [25]. Therefore, the broadening due to the rf induced shifts does alter the short term stability and having 10 or 20 ions instead of one effectively results in a gain in stability by \sqrt{N} .

Furthermore, the fluctuations of the rf induced effects over long time scales are not the limiting factors for the long term stability of the clock. Indeed, a single ion standard encoun-

TABLE I: Uncertainty budget for the frequency transition of $|S_{1/2}, M_J = \pm 1/2\rangle \rightarrow |D_{5/2}, M_J = \mp 1/2\rangle$ in $^{40}\text{Ca}^+$, based on a ring in an octupole linear trap with $\omega_z/2\pi = 1$ MHz, $\Omega/2\pi = 20$ MHz, and a rf electric field such that $R = 20\mu\text{m}$ (10 ions) or $40\mu\text{m}$ (20 ions), as given in the table.

effect	conditions	shift (Hz)	broadening	long term instability
Doppler(2^e)	$R = 20\mu\text{m}$	+6.0	± 0.14	8×10^{-17}
	$R = 40\mu\text{m}$	+24.1	± 0.28	5×10^{-17}
Stark	$R = 20\mu\text{m}$	+4.1	± 0.09	6×10^{-17}
	$R = 40\mu\text{m}$	+16.5	± 0.19	3×10^{-17}
Zeeman	$\delta B \leq 6 \times 10^{-7}$ G		< 1	2.5×10^{-15}
BBR	$T = 300 \pm 10$ K	$+0.38(1) \pm 0.05$		$< 10^{-16}$
quadrupole	trapping field	+8.0	< 0.1	$\leq 10^{-17}$
quadrupole	extra dc		$\simeq 0.04$	$\leq 10^{-16}$
total	$R = 20\mu\text{m}$	+18.5	± 0.2	2.5×10^{-15}
total	$R = 40\mu\text{m}$	+49.0	± 0.4	2.5×10^{-15}

ters the same limitations concerning uncertainty and long term stability, due to coupling to the local electric and magnetic fields. The challenge for a ring is to keep the stability constrains over larger spatial scales than for a single ion.

As we have seen earlier, increasing the number of trapped ions allows to further reduce the long term fluctuations induced by ion loss, which scale like $\delta N/N^3$ and to lower the short term instability by increasing the signal to noise ratio. In this article, we limited our study to 10 and 20 ions ring to keep the temperature compatible with clock operation conditions while the cooling lasers are off. An alternative to a sequential operation that could allow to work with larger rings is to sympathetically cool the calcium ions by ions with a different mass (LC ions). Our MD simulations on 10 calcium ions show that conditions for axial and radial decoupling can be found, allowing the LC ions to reach their Doppler limit on the axial motion while calcium axial temperature fluctuates between 1 and 3 mK. These studies have to be extended [33] to larger samples to demonstrate a gain compared to the simple one species ring we have considered in this article. Such large cold rings could find an interest in metrology and/or quantum information or simulation. With today's state of the art in magnetic field stabilisation, the ion loss is not the limiting effect for the frequency stability of a clock based on a ring of ions and this configuration can offer the possibility to test many particles system for metrology.

Acknowledgments

One of the authors (C.C.) thanks Tanja Mehlstäubler for stimulating discussions about the ring configuration. Fernande Vedel is gratefully acknowledged for her suggestions. M. Kajita was supported by a visiting professor grant at the Université de Provence when part of this work was initiated.

-
- [1] T. Udem, S. A. Diddams, K. R. Vogel, C. W. Oates, E. A. Curtis, W. D. Lee, W. M. Itano, R. E. Drullinger, J. C. Bergquist, and L. Hollberg, *Phys. Rev. Lett.* **86**, 4996 (2001).
 - [2] C. Degenhardt, H. Stoehr, C. Lisdat, G. Wilpers, H. Schnatz, B. Lipphardt, T. Nazarova, P.-E. Pottie, U. Sterr, J. Helmcke, et al., *Phys. Rev. A* **72**, 062111 (2005).
 - [3] M. Takamoto, F.-L. Hong, R. Higashi, and H. Katori, *Nature* **435**, 321 (2005).
 - [4] T. Akatsuka, M. Takamoto, and H. Katori, *Nature Physics* **4**, 954 (2008).
 - [5] N. D. Lemke, A. D. Ludlow, Z. W. Barber, T. M. Fortier, S. A. Diddams, Y. Jiang, S. R. Jefferts, T. P. Heavner, T. E. Parker, and C. W. Oates, *Phys. Rev. Lett.* **103**, 063001 (2009).
 - [6] H. S. Margolis, G. P. Barwood, G. Huang, H. A. Klein, S. N. Lea, K. Szymaniec, and P. Gill, *Science* **306**, 1355 (2004).
 - [7] A. A. Madej, J. E. Bernard, P. Dubé, L. Marmet, and R. S. Windeler, *Phys. Rev. A* **70**, 012507 (2004).
 - [8] T. Schneider, E. Peik, and C. Tamm, *Phys. Rev. Lett.* **94**, 230801 (2005).
 - [9] T. Rosenband, D. B. Hume, P. O. Schmidt, C. W. Chou, A. Brusch, L. Lorini, W. H. Oskay, R. E. Drullinger, T. M. Fortier, J. E. Stalnaker, et al., *Science* **319**, 1808 (2008).
 - [10] P. Fisk, *Rep. Prog. Phys.* **60**, 761 (1997).
 - [11] J. Prestage, S. Chung, T. Le, L. Lim, and L. Maleki, in *Proceedings of IEEE Int. Freq. Contr. Symp. Miami, jun. 5-7, 2006* (IEEE, New York, 2006).
 - [12] J. Prestage and G. Weaver, *Proceeding of the IEEE* **95**, 2235 (2007).
 - [13] J. Prestage, R. Tjoelker, and L. Maleki, *Proceedings of the 1999 Joint EFTF-IFCS, Besancon, France* pp. 121–124 (1999).
 - [14] J. Prestage, R. Tjoelker, and L. Maleki, *Frequency measurement and control: Advanced techniques and future trends* (Springer, Berlin, 2001), chap. Recent developments in microwave ion clocks.
 - [15] D. Gerlich, in *State-selected and state-to-state ion-molecule reaction dynamics, Part I*, edited by C.-Y. Ng and M. Baer (John Wiley and Sons, 1992), vol. 82 of *Advances in Chemical Physics Series*.

- [16] R. Wester, J. Phys. B **42**, 154001 (2009).
- [17] K. Okada, K. Yasuda, T. Takayanagi, M. Wada, H. A. Schuessler, and S. Ohtani, Phys. Rev. A **75**, 033409 (2007).
- [18] K. Okada, T. Takayanagi, M. Wada, S. Ohtani, and H. A. Schuessler, Phys. Rev. A **80**, 043405 (2009).
- [19] F. Calvo, C. Champenois, and E. Yurtsever, Phys. Rev. A **80**, 063401 (pages 6) (2009).
- [20] C. Champenois, J. Phys. B **42**, 154002 (2009).
- [21] W. Itano, J. Bergquist, J. Bollinger, J. Gilligan, D. Heinzen, F. Moore, M. Raizen, and D. Wineland, Phys. Rev. A **47**, 3554 (1993).
- [22] D. Porras and J. I. Cirac, Phys. Rev. Lett. **96**, 250501 (2006).
- [23] I. M. Buluta, M. Kitaoka, S. Georgescu, and S. Hasegawa, Phys. Rev. A **77**, 062320 (2008).
- [24] B. Olmos, R. González-Férez, and I. Lesanovsky, Phys. Rev. Lett. **103**, 185302 (2009).
- [25] C. Champenois, M. Houssin, C. Lisowski, M. Knoop, M. Vedel, and F. Vedel, Phys. Lett. A **331**, 298 (2004).
- [26] M. Kajita, Y. Li, K. Matsubara, K. Hayasaka, and M. Hosokawa, Phys. Rev. A **72**, 043404 (2005).
- [27] E. Teloy and D. Gerlich, Chemical Physics **4**, 417 (1974).
- [28] J. Mikosch, U. Fröhling, S. Trippel, R. Otto, P. Hlavenka, D. Schwalm, M. Weidemüller, and R. Wester, Phys. Rev. A **78**, 023402 (pages 13) (2008).
- [29] J. Mikosch, U. Fröhling, S. Trippel, D. Schwalm, M. Weidemüller, and R. Wester, Phys. Rev. Lett. **98**, 223001 (2007).
- [30] M. G. Raizen, J. M. Gilligan, J. C. Bergquist, W. M. Itano, and D. J. Wineland, Phys. Rev. A **45**, 6493 (1992).
- [31] W. Itano, I. Lewis, and D. Wineland, Phys. Rev. A **25**, 1233 (1982).
- [32] D. J. Wineland and W. M. Itano, Phys. Rev. A **20**, 1521 (1979).
- [33] M. Marcianti and *et. al*, in preparation.
- [34] W. Itano, J. Res. Natl. Inst. Stand. Technol. **105**, 829 (2000).
- [35] B. Arora, M. S. Safronova, and C. W. Clark, Phys. Rev. A **76**, 064501 (2007).
- [36] E. A. Burt, J. Prestage, and R. Tjoelker, Proceedings of the IEEE IFCS, New Orleans p. 463 (2002).
- [37] C. Roos, M. Chwalla, K. Kim, M. Riebe, and R. Blatt, Nature **443**, 316 (2006).
- [38] D. Jiang, B. Arora, and M. S. Safronova, Phys. Rev. A **78**, 022514 (2008).
- [39] N. Kjærgaard, L. Hornekaer, A. M. Thommesen, Z. Videsen, and M. Drewsen, Appl. Phys. B **71**, 207 (2000).
- [40] S. Gulde, D. Rotter, P. Barton, F. Schmidt-Kaler, R. Blatt, and W. Hogervorst, Appl. Phys.

- B **73**, 861 (2001).
- [41] P. Dubé, A. A. Madej, J. E. Bernard, L. Marmet, J.-S. Boulanger, and S. Cundy, Phys. Rev. Lett. **95**, 033001 (2005).
- [42] D. Wineland, J. Bollinger, W. Itano, and D. Heinzen, Phys. Rev. A **50**, 67 (1994).